Energy Conversion and Management 52 (2011) 97–107

Contents lists available at ScienceDirect

Energy Conversion and Management

journal homepage: www.elsevier.com/locate/enconman

A numerical analysis of an active magnetic regenerative refrigerant system with a multi-layer regenerator

C. Aprea [a], A. Greco [b,*], A. Maiorino [a]

[a] Dipartimento di Ingegneria Meccanica, Università di Salerno, Via Ponte Don Melillo, 84084 Fisciano, SA, Italy
[b] DETEC, Università degli Studi di Napoli Federico II, P.le Tecchio 80, 80125 Napoli, Italy

ARTICLE INFO

Article history:
Received 2 September 2009
Received in revised form 7 June 2010
Accepted 22 June 2010
Available online 9 August 2010

Keywords:
Magnetic refrigeration
AMRR cycle
Layered bed
Gd_{-x} Tb_{1-x} alloys
Gd_{-x} Dy_{1-x} alloys

ABSTRACT

Magnetic refrigeration is an emerging technology based on the magnetocaloric effect in solid-state refrigerants.

The active magnetic regenerative refrigeration (AMRR) cycle is a special kind of regenerator for the magnetic refrigerator, in which the magnetic material matrix works both as a refrigerating medium and as a heat regenerating medium, while the fluid flowing in the porous matrix works as a heat transfer medium. The performance of an AMRR cycle depends strongly on the behaviour of the adiabatic magnetization temperature change as a function of material temperature in the flow direction of the regenerator.

In the present paper, a practical model for predicting the performance and efficiency of an AMRR cycle has been developed. The model simulates both the ferromagnetic material and the entire cycle of an AMRR operating in conformity with a Brayton regenerative cycle. The model simulates different kinds of layered regenerators operating at their optimal operation point. The program study the Gd_{-x} Tb_{1-x} alloys as constituent materials for the regenerator over the temperature range 275–295 K, and Gd_x Dy_{1-x} alloys in the temperature range 260–280 K. With this model, the refrigeration capacity, the power consumption and consequently the coefficient of performance can be predicted. The results show a greater COP for the refrigerator based on the magnetocaloric technology compared with the COP of a classical vapour compression plant working between the same thermal levels.

1. Introduction

Magnetic refrigeration is an emerging technology based on the magnetocaloric effect in solid-state refrigerants [1,2]. In the case of ferromagnetic materials the magnetocaloric effect (MCE) is a warming as the magnetic moments of the atom are aligned by the application of a magnetic field, and the corresponding cooling upon removal of the magnetic field.

Compared to conventional vapour compression systems, magnetic refrigeration can be an efficient and environmentally friendly technology. The high efficiency arises because the analogues to the compression and expansion parts of the vapour compression cycle are accomplished by the magnetization and demagnetization of a magnetic material. Furthermore, the magnetic refrigerant is a solid and has essentially zero vapour pressure and therefore is ecologically sound with no Ozone Depletion Potential (ODP) and zero direct Global Warming Potential (GWP) [3].

The magnetic field of magnetic refrigeration can be supplied by electromagnet, superconductor or permanent magnet, which has no need for compressors with movable components, large rotational speed, mechanical vibration noise, bad stability and short longevity.

Recently, the research for magnetic refrigeration working materials has been greatly expanded. In this paper attention is focused in the near room temperature MCE.

A good material for the refrigeration at room temperature is gadolinium, which is a member of the lanthanide group of elements. At the Curie temperature T_C of 294 K, Gd undergoes a second order paramagnetic – ferromagnetic phase transition. Dan'kov et al. [4] first studied the magnetocaloric properties of high-purity Gd and found the maximum adiabatic temperature change during magnetization, ΔT_{ad}, to be approximately 5.8 K when magnetized from 0 to 2 T. They also founded an entropy change with magnetization of −5.5 J/kg K. They reported also that there was no detectable magnetic hysteresis in single gadolinium crystals. The thermal conductivity of Gd near room temperature is approximately 10 W/m K [5].

A variety of Gd–R alloys, where *R* is another lanthanide metal have been prepared in an attempt to improve the MCE in Gd. Gd can be alloyed with terbium (Tb) [6], dysprosium (Dy) [7], or erbium (Er) [8] to lower the Curie temperature in order to construct a layered regenerator.

* Corresponding author. Tel.: +39 0817682289; fax: +39 0812390364.
E-mail address: adriana.greco@unina.it (A. Greco).

0196-8904/$ - see front matter © 2010 Elsevier Ltd. All rights reserved.
doi:10.1016/j.enconman.2010.06.048

Nomenclature

Symbols

A	heat transfer surface, m^2
B	magnetic induction, T
B_j	Brillouin function
c	specific heat, J/kg K
COP	coefficient of performance
D	diameter of the regenerator section, m
d_p	diameter of the particles, m
g_j	Landè factor
h	heat transfer coefficient, W/m^2K
J	total angular momentum quantum
K	Boltzman constant. J/K
k	thermal conductivity, W/mK
L	length of the regenerator, m
M	magnetization, A/m
M_m	molar mass, kg/mol
m	mass, kg
N	number of atoms per volume, $1/m^3$
Na	number of atoms per molecule
p	pressure, Pa
Q	thermal energy, J
R	universal constant gas, J/mol K
S	entropy, J/K
s	specific entropy, J/kg K
T	temperature, K
t	time, s
v	specific volume, m^3/kg
W	work, J
w	local velocity, m/s
x	space, m
x	mass fraction of Gd

Greek symbols

γ	electronic constant, J/K mol
Δ	finite difference, –
δ	error, K
ε	porosity, –
η	isentropic efficiency, –
μ	viscosity, Pa s
μ_B	Bohr magneton, J/T

Subscripts

ad	adiabatic
B	magnetic field constant
b	bed
C	Curie
c	cold
CF	cold water flow
D	demagnetization phase
De	Debye
el	electronic
f	fluid
h	hot
inf	undisturbed flow
HF	hot water flow
lat	lattice
M	magnetization phase
m	magnetic
max	maxim
M.C.	Carnot machine
p	particle
ref	refrigeration
rej	reject
tot	total
tr	trial

The main objective of this paper is to investigate the effect of different temperature profile on the refrigeration capacity and on the efficiency of the AMRR cycle. To this hope, a practical model for predicting the refrigeration capacity and the efficiency of an AMRR cycle has been developed.

The Gd–Dy alloys have been chosen as constituent materials for the regenerators operating over the temperature range 260–280 K, whereas, the Gd–Tb alloys have been chosen as constituent materials for the regenerators operating over the temperature range 275–295 K. The regenerator's compositions have been determined numerically and their thermomagnetic properties have been calculated using the molecular field theory and the Debye approximation. These materials have a very convenient property to produce layered beds, namely that the Curie temperature changes with the fraction of change of two components. Therefore, a pure gadolinium regenerator exhibits a large magnetocaloric effect only over a small temperature range containing its Curie temperature. Using alloys it is possible to fabricate a layered bed composed of several magnetic alloys, each placed at the location in the regenerator where the average temperature is near its Curie temperature.

2. A state of the art on magnetic refrigeration

The study of magnetic refrigeration was started with the discovery of magnetocaloric effect (MCE) 120 years ago [9]. Then it has been used in cryogenic refrigeration since 1930s. It is maturely used in liquefaction of hydrogen and helium. In 1976, at Lewis Research Centre of American National Aeronautics and Space Administration, Brown first applied the magnetic refrigeration in room temperature range [10]. By employing gadolinium (Gd) as the magnetic working substance, he attained a 47 K no-load temperature difference in a 7 T magnetic field.

Essential for the design of an AMR cycle is the magnetic field generation. The magnetic field can be generated by a permanent magnet or an electromagnet. The upper limit of the magnetic field strength that can be achieved using a permanent magnet today is approximately 2 T. Magnetic field up to 2 T can be applied by an electromagnet. Within the electromagnets superconducting electromagnets can be also used. These consist in electromagnets cooled in order to reach very low temperature. In this temperature range the superconductivity can be utilized for magnetic field generation.

Different mechanical realizations of AMRR cycles are possible and several prototype systems have been constructed. Most of the regenerators of the experimental plants are made of gadolinium. Some of these prototypes have implemented layered regenerators beds with gadolinium based alloys. Only few regenerators are made with magnetic materials with first order transition phase.

A summary of the most significant prototype systems developed is reported in Table 1. In this table the origin of the research group, the kind of relative motion between the magnet and the regenerator, the maximum magnetic field, the regenerator's volume, the frequency of the magnetization/demagnetization process, the magnetic material, the cooling power, the temperature span of the system, the regenerator geometry, the reference are specified.

The University of Victoria prototype consists of two regenerators beds that are moved linearly through a magnetic field that is

Table 1
Summary of the experimental AMRR systems.

Research group	Conf.	μ_oH (T)	N° beds	Reg. vol. (cm^3)	Freq. (Hz)	Regen. material	Qc (W)	ΔT (K)	Regen. Geom.	Ref.
US Navy	Alter.	7 (E)	1	173	0.01	Gd	0	40	Ribbon (0.2 mm)	[11]
Univ. Vittoria	Alter.	2(S)	2	74	1	Gd	0	50	Crushed part. (0.25–0.65 mm) spheres (0.2 mm)	[12–14]
		2(S)		74	1	GdTb	0	50		
		2(S)		74	1	GdEr	0	50		
		2(S)		49	0.8	Gd	0	15.5		
		2(S)		25	0.6	Gd	7	14		
Chubu electric/Toshiba	Alter.	4(S)	2	484	0.167	Gd	100	26	Spheres (0.3 mm)	[15]
		2(S)					40	24		
Austr.	Alter.	5(S)	2	600	0.167	Gd	100	38	Spheres (0.15–0.3 mm)	[16]
							600	0		
Austr.	Rotat.	1.5 (P)	6	33	4	Gd	15	14	Spheres (0.43–0.5 mm) spheres (0.25–0.4 mm)	[17]
						GdEr	27	14		
							0	25		
Austr.	Rotat.	1.5 (P)	12	242	2	Gd	220	0	Plates	[18]
							155	8		
Grenoble	Alter.	0.8 (P)	1	32	0.42	Gd	9	4	Plates	[19]
Nanjing University	Alter.	1.4 (P)	2	200	0.25	Gd	0	23	Spheres (0.2 mm)	[20]
						$Gd_5Si_2Ge_2$	0	10		
						GdSiGeGa	0–40	25–5		
Tokyo institut of techology/ Chubu	Rotat.	1.1 (P)	4	844	0.39	GdDy	540	0.2	Spheres (0.5 mm)	[21]
					0.42		150	5.2		
Xi'an Jiaotong University	Alter.	2.2(S)	1	200	0.1	Gd	19	4	Spheres (0.15–0.3 mm) part. (0.3–0.75 mm)	[22–23]
						$Gd_5Si_2Ge_2$	10	3		

N.B. μ_oH: *S*, superconducting magnet; *E*, elettromagnet; *P*, permanent magnet.

generated by a stationary superconducting solenoid magnet (maximum field of 5 T). The heat transfer fluid is helium and the regenerator is made of Gd and its alloys (multi-layer bed). Using a Gd bed, the prototype produced 7 W of cooling power. A no-load temperature span of 51 K is achieved with a multi-layer bed.

The Chubu/Toshida AMRR has two regenerator beds that are moved linearly in the presence of a magnetic field that is generated by a superconducting solenoid (with a magnetic field variable between 2 and 4 T). The heat transfer fluid is a mixture of water and ethanol. The cooling power is 100 W with a COP of 5.6 when the system operates between 276 and 302 K. However, the reported COP is somewhat misleading because it does not include the work pump that move the secondary fluid and also neglects the power that is required to cool the superconducting solenoid.

Astronautics Corporation of America' s first near room temperature AMRR prototype was a reciprocating device with a 5 T magnetic field generated by a superconducting solenoid. Two regenerators were made of Gd. A cooling power of 100 W was achieved from his device with a temperature span of 38 K. Although the original device produced a relatively large cooling power over a large temperature span, the device itself was quite large and uses a superconducting magnet and therefore would not be practical as a commercial product.

Astronautics has recently built a new device that uses a more practical, 1.5 T permanent magnet. The device uses a rotating regenerator divided into six separated beds. The regenerator is made of single magnetic material (Gd and LaFeSiH) and of different materials arranged in a multi-layer configuration (Gd–Er alloys). The cooling power, with a temperature span of 14 K, is 15 W with the Gd regenerator and 27 W with a multi-layer bed. The regenerator bed made of LaFeSiH material produces a lower cooling power.

A more recent rotary device that uses a rotating permanent magnet with 12 stationary bed made of Gd has been built. Experimental tests report cooling powers of 155 and 220 W with a temperature span of 8 K.

Nanjing University built a reciprocating device consisting of two regenerator beds moving linearly into and out of the magnetic field generated by a stationary 1.4 T permanent magnet. The beds are made of Gd and with first order magnetic materials (GdSiGeGa and GdSiGe). The experimental results report a no-load temperature span of 23 K with Gd, 25 K with GdSiGeGa and 10 K with GdSiGe.

The Tokyo Institute of Technology system is a rotary device that uses a rotating magnet with a stationary regenerator made of Gd–Dy alloys. The permanent magnet produces a magnetic field of 1.1 T. The system produces a cooling load of 150 W with a temperature span of 5.2 K.

The Xi'an Jiaotong University built a reciprocating AMRR with a single regenerator bed that uses a 2.18 T electromagnet. The regenerator's bed is made of Gd and GdSiGe alloys. The cooling power is 18.7 W with a Gd bed and 10.3 W with the first order magnetic material bed with a temperature span of 3 K.

Different mechanical realizations of the AMRR cycle are possible and several prototype systems have been constructed. Nevertheless, in many experimental devices the magnetic field is generated by means of an electromagnet or of a superconducting electromagnet. However these configurations are not of practical interest because of the large currents that are required to generate useful magnetic fields for an electromagnet and because of the power required by cryogenic equipment necessary to maintain the superconducting temperature of a solenoid magnet (this power can greatly exceed the cooling power of small to medium scale AMRR device). These configurations are therefore applicable only in the cryogenic temperature range. Applications in the room temperature field are possible only with a permanent magnet to generate a magnetic field. Between the experimental devices developed,

most of them have low cooling power and low energetic performances and therefore are not useful for practical applications. Therefore attention should be paid on the development of a new experimental prototype characterized by a greater cooling power (for commercial applications) and by energetic performances greater than those of a traditional vapour compression plant.

To this aim an optimal regenerator must be designed. This goal can be achieved utilizing an optimum magnetocaloric refrigerant and an optimum exchange fluid. A larger MCE in refrigerant material results in a greater change of internal energy and provides more cooling that needs to be transferred out of the bed by the exchange fluid. The regenerator can be made with a first or a second order material. The first order materials exhibit a giant magnetocaloric effect but three major problems arise in their use: (1) in a first order magneto structural transition a large volume change occurs; (2) large hysteresis; and (3) a finite time for the adiabatic temperature variation to reach its maximum equilibrium value [24].

One method to span the temperature range is to choose several second order transition alloys and arrange them in the regenerator from the cold end to the hot end in a multi-layer arrangement.

The secondary fluid behaviour is a major fact that can improve the performance of an AMRR system. Therefore nature of the exchange fluid can perform an important task in heat transfer through the regenerative bed.

The development of a mathematical model allow to find an optimal configuration so that to be able to build subsequently an experimental prototype. To this hope, a practical model for predicting the refrigeration capacity and the efficiency of an AMRR multi-layer cycle has been developed in this paper. The alloys have been chosen in such a way that their Curie point follows the regenerator temperature profile. This model is flexible with regard to modelling inputs such as regenerator geometry, fluid flow profile, variations in magnetic field, and material properties. This model enables also the valuation of the best secondary fluid in different temperature ranges.

Different analytical model have been developed in order to evaluate the potential of an AMRR cycle. Most of them are mono-dimensional with gadolinium as magnetic material and water as a secondary fluid. In the follow reference will be made to the more recent models.

Engelbrecht et al. have presented a one-dimensional model using as magnetic material gadolinium and its alloys and as secondary fluid water [25,26].

Rowe et al. [27] developed a numerical model using as magnetic material for the simulation Gd and $DyAl_2$. This Research group study with a mathematical model demagnetizing effect in a single-material AMRR [28,29].

A time and spatially dependent model was developed by Shir et al. [30]. The magnetic material was gadolinium and the secondary fluid a gas.

In the paper of Bouchekara et al. [31,32] an inverse approach is considered. Starting from the system performance required they developed an optimization process based on an AMRR model. The magnetic material was gadolinium, the secondary fluid water.

Two and three dimensional models have been also presented [33–35]. Most of them are for flat plate regenerators. For these models the computation time may be prohibitive and the possibility of varying the regenerator geometry is limited. A comparison between the mono-dimensional and two dimensional models show excellent agreement for packed sphere regenerators and for flat parallel plates regenerators with thin regenerator channels [36].

3. Magnetocaloric regeneration

Two major difficulties arise in the design of a magnetic refrigeration system. First, the magnetocaloric effect is fairly small in room temperature applications. Second, the refrigerant is solid, and thus cannot be pumped in the heat exchangers. The problem of heat transfer and of temperature span can be overcome with the introduction of the heat transfer fluid and of regeneration. Regeneration can be accomplished by blowing the heat transfer fluid in reciprocating fashion through a porous bed of magnetocaloric material that is alternately magnetized and demagnetized.

The active magnetic regenerative refrigeration (AMRR) cycle is a special kind of regenerator for the magnetic refrigerator, in which the magnetic material matrix works both as a refrigerating medium and as a heat regenerating medium, while the fluid flowing in the porous matrix works as a heat transfer medium. An active magnetic regenerator can provide larger temperature spans with adequate heat transfer between the regenerator matrix and fluid. An AMRR cycle consists of the four following processes: (1) bed magnetization; (2) iso-field cooling; (3) bed demagnetization; and (4) iso-field heating.

Initially the porous regenerator bed is at a steady state condition with the hot heat exchanger at T_h and the cold heat exchanger at T_c. In the magnetization process, the magnetic field in the bed is increased with no fluid flow, which causes the temperature of material to increase due to the magnetocaloric effect. The temperature of the magnetic material at the hot end of the bed rises above the hot heat exchange temperature T_h. In the iso-field cooling process, with the high magnetic field, the fluid is blown from the cold end to the hot end of the bed. The magnetic material temperature decreases because the fluid absorbs heat from the bed and after expel heat at a temperature higher than T_h in the hot heat exchanger. In the bed demagnetization process the magnetic material temperature decreases with no fluid flow. Finally, in the last step, with a zero field, the fluid is blown from the hot end to the cold end of the bed. The magnetic material temperature increases because the fluid expels heat to the bed and after absorbs heat at a temperature lower than T_c in the cold heat exchanger, producing the cooling load.

In the AMRR each particle of the magnetic material in the packed bed undergoes a unique magnetic Brayton cycle and the whole bed undergoes a cascade Brayton cycle, so that the temperature span can greatly exceed the adiabatic temperature change of magnetic refrigerant.

4. The mathematical model

In order to analyze and design an optimum magnetic refrigeration system, it is important to model the magnetization and demagnetization process of the magnetic material and the regenerative warm and cold blow processes. The initial and the boundary conditions of each process connect each step of the four sequential processes to allow a cyclical operation of the AMRR system.

4.1. The model of magnetization and demagnetization processes

A homogeneous ferromagnetic material model has been used to characterize the thermal and magnetic behaviours. The basic thermodynamics of the MCE is well known [37]. An entropy balance for the magnetocaloric solid refrigerant and the entrapped fluid in the porous matrix has been performed [38]:

$$dS = m_b \frac{c_b}{T_b} dT_b + \nu_b m_b \left(\frac{\partial M}{\partial T_b}\right)_H dB + m_f ds_f \quad (1)$$

To study the transient behaviour, ignoring the mass of the entrapped fluid compared to the mass of the magnetic material, the temperature variation is valuable integrating the following differential equation:

$$\left(\frac{\partial T_b}{\partial t}\right)_x = -\frac{T_b}{c_b}\nu_b\left(\frac{\partial M}{\partial T_b}\right)_H \frac{dB}{dt} \quad (2)$$

The derivative of the magnetization in respect to the temperature at constant magnetic field, is obtainable numerically by the function $M(B, T)$ provided by the ferromagnetic homogeneous model. A simplified molecular theory allows the $f(B, M, T) = 0$ state equation reported below for the magnetization [39]:

$$M(B,T) = Ng_J\mu_B J B_J(X) \quad (3)$$

where:

$$B_J(X) = \frac{2J+1}{J}\coth\left(\frac{2J+1}{2J}X\right) - \frac{1}{2J}\coth\left(\frac{X}{2J}\right) \quad (4)$$

is the Brillouin function based on the theory of the medium field of a magnetic material derived by a statistical approach and:

$$X = g\mu_B J\frac{B+\lambda M}{kT} \quad (5)$$

where λ is the Curie constant:

$$\lambda = \frac{3K}{Ng^2\mu_B^2 J(J+1)}T_C \quad (6)$$

At constant pressure, the entropy of a magnetic solid can be expressed as the sum of the magnetic, lattice and electronic contributions:

$$S(T,B) = S_m(T,B) + S_{lat}(T) + S_{el}(T) \quad (7)$$

The magnetic entropy is equal to:

$$s_m(B,T) = \frac{R}{M_m}\left[\ln\frac{\sinh\left(\frac{2J+1}{2J}X\right)}{\sinh\left(\frac{X}{2J}\right)} - XB_J(X)\right] \quad (8)$$

The vibration electronic entropy is equal to:

$$s_{el}(T) = \frac{\gamma}{M_m}T \quad (9)$$

The last contribution to the entropy can be expressed as:

$$s_{lat}(T) = \frac{N_a R}{M_m}\left[-3\ln\left(1-e^{\frac{T_{De}}{T}}\right) + 12\left(\frac{T_{De}}{T}\right)^3\int_0^{\frac{T_{De}}{T}}\frac{z^3}{e^z+1}dz\right] \quad (10)$$

It is possible to obtain the specific heat versus the temperature at constant magnetic field, according the Maxwell equation:

$$c_b(B,T) = T\left(\frac{\partial s}{\partial T}\right)_B \quad (11)$$

Comparing the numerical results for Gd [40] obtained with theoretical model and experimental results supplied by others [41,42], a good compromise has been found. The values of the specific heat calculated in this study are comprised the theoretical values indicated by Yu et al. [42], and the experimental ones reported by Peksoy and Rowe [41]. The oscillations are apparently due to both the different values used for the characteristics constants in the calculus of the specific heat and to the impurity of the materials used for experiments.

The values for Gd, Dy, and Tb parameters g, J, M_m, T_C, and T_{De} used in the calculations are presented in Table 2.

From these data, the parameters of the different $Gd_x\ Dy_{1-x}$ and of the different $Gd_x\ Tb_{1-x}$ alloys, varying the composition, can be evaluated by interpolation and considering the following relationships:

Table 2
Magnetic and thermal parameters of Gd, Dy, and Tb.

Element	g	J	M_m (kg/mol)	T_C (K)	T_{De} (K)
Gd	2	3.5	0.157	294	173
Dy	1.33	7.5	0.163	179	180
Tb	1.5	6	0.159	230	177

$$\overline{G} = xG_{Gd} + (1-x)G_{Tb} \quad (12)$$

$$\overline{G} = xG_{Gd} + (1-x)G_{Dy} \quad (13)$$

$$\bar{\mu}^2 = x\mu_{Gd}^2 + (1-x)\mu_{Tb}^2 \quad (14)$$

$$\bar{\mu}^2 = x\mu_{Gd}^2 + (1-x)\mu_{Dy}^2 \quad (15)$$

where G is the De Gennes factor and is defined as:

$$G = (g-1)^2 J(J+1) \quad (16)$$

And μ is the effective magnetic moment defined as:

$$\mu = g\sqrt{J(J+1)} \quad (17)$$

Therefore from Eqs. (16) and (17) one can deduce the corresponding g and J for a given alloy. The Curie temperature of the alloy is evaluated as:

$$\overline{T}_C = 46\overline{G}^{2/3} \quad (18)$$

Smaili and Chahine [43] show in their paper this model for Gd–Dy alloys. A comparison between the numerical data obtained with the de Gennes model and the experimental values of the Curie temperature and of the isothermal magnetic entropy variation of the alloy Gd_xTb_{1-x} has been performed [44,45]. The comparison shows satisfactory agreement.

4.2. The model of the regenerative warm and cold blow processes

The choice of the secondary fluid is very important to improve the energetic performances of the AMRR system. The secondary fluids in the simulation are: water–monoethylenglycol mixture (50% by weight), water–monoethylenglycol mixture (34% by weight) and water-1,2 propylenglycol mixture (38% by weight) in the 260–280 K temperature range; pure water in the 275–295 K range.

The analysis and equations in this section are based on the following simplifying assumptions:

1. The temperature of the secondary fluid entering at each end of the refrigerant bed is constant. The secondary fluid exchanges thermal energy with the environment thanks to two heat exchangers not considered in the present mathematical model. The heat exchangers are expected to be very efficient (with an infinite heat exchange area), such that the secondary fluid alternatively flowing from the heat exchangers into the refrigerant bed is cooled until a temperature of T_h and is heated until a temperature of T_c.
2. The axial conduction in the magnetic bed is assumed negligible.
3. The bed is assumed adiabatic towards the environment.
4. The properties of the magnetic material are assumed constant throughout the bed.
5. The secondary fluid is considered incompressible.
6. The secondary fluid velocity is constant during the period of flow blowing.
7. The fluid flow through the bed is parallel and uniform throughout any cross section. The temperature change perpendicular to the main flow direction can be therefore neglected and the problem can be considered one-dimensional.
8. The fluid pressure drop throughout the bed has been neglected.

9. The regenerator surface area is evenly distributed throughout its volume.

Based on the above assumptions, an energy balance for the secondary fluid and for the magnetic material can be performed, which results in two partial differential equations:

$$\begin{cases} m_f c_f \frac{\partial T_f}{\partial t} + \dot{m}(t) L c_f \frac{\partial T_f}{\partial x} = hA(T_b - T_f) \\ m_b c_b \frac{\partial T_b}{\partial t} = hA(T_f - T_b) \end{cases} \quad (19)$$

To evaluate the heat transfer coefficient for the water the Roshenow correlation [46] has been considered.

4.3. The boundary and the initial conditions of the refrigeration cycle

The boundary and initial conditions for the Eqs. (2) and (19), will present below for each phase of the cycle. It is useful to explain each phase of the refrigeration cycle starting from the phase of demagnetization. In demagnetization, at $t = 0$, the bed is subjected to a magnetic field B_{max}. The magnetic field is nullified, according to the function $B(t)$, at $t = t_D$. Using the Eq. (2) with the initial condition:

$$T_b(0,x) = T_{b,HF}(x) \quad (20)$$

a new temperature profile is obtained:

$$T_{b,D}(x) = T_b(t_D,x) \quad (21)$$

In the last step ($t_D \leqslant t \leqslant, t_{CF}$) in the absence of the magnetic field, the fluid is blown from the hot end to the cold end of the bed. The secondary fluid enters the hot side of the bed at temperature equal to T_h. The secondary fluid contained in the bed at the time $t = t_D$ presents the same temperature profile reached at the time $t = t_D + t_{CF} + t_M + t_{HF}$. Considering the Eq. (19) with the following initial and boundary conditions:

$$\dot{m}(t) = -\dot{m}_0 \quad (22)$$
$$T_f(t_D,x) = T_{f,HF}(x) \quad (23)$$
$$T_f(t,L) = T_h \quad (24)$$
$$T_b(t_D,x) = T_{b,D}(x) \quad (25)$$

the new temperature profiles for the bed and for the regenerating fluid are determined:

$$T_{b,CF}(x) = T_b(t_D + t_{CF},x) \quad (26)$$
$$T_{f,CF}(x) = T_f(t_D + t_{CF},x) \quad (27)$$

In the magnetization phase ($t_{CF} \leqslant t \leqslant t_M$), the bed is magnetized increasing the magnetic field, until B_{max}, according to a linear evolution.

Using the Eq. (2) with the following initial condition:

$$T_b(t_D + t_{CF},x) = T_{b,CF}(x) \quad (28)$$

a new temperature profile of the bed is obtained:

$$T_{b,M}(x) = T_b(t_D + t_{CF} + t_M,x) \quad (29)$$

In the fourth phase ($t_M \leqslant t \leqslant t_{HF}$), the fluid is blown from the cold end to the hot end of the bed. The magnetic field is equal to B_{max} and the secondary fluid in the bed exhibits the same profile temperature showed at the time $t = t_D + t_{CF}$. The regenerating fluid passes through the bed entering at its cold side at temperature equal to T_C. Considering the Eq. (19) and the following initial and boundary conditions:

$$\dot{m}(t) = \dot{m}_0 \quad (30)$$
$$T_f(t_D + t_{CF} + t_M,x) = T_{f,CF}(x) \quad (31)$$
$$T_f(t,0) = T_c \quad (32)$$
$$T_b(t_D + t_{CF} + t_M,x) = T_{b,M}(x) \quad (33)$$

the new temperature profiles for the bed and for the regenerating fluid are determined:

$$T_{b,HF}(x) = T_b(t_D + t_{CF} + t_M + t_{HF},x) \quad (34)$$
$$T_{f,CF}(x) = T_f(t_D + t_{CF} + t_M + t_{HF},x) \quad (35)$$

4.4. Numerical solution

There is not analytical solution to solve for the equations presented previously. The Runge–Kutta explicit method has been used to solve the equations system. Because the model concerns a thermodynamic cycle two conditions have to be respected:

$$T_B(0,x) = T_B(t_D + t_{CF} + t_M + t_{HF},x) \quad (36)$$
$$0 < COP < COP_{M.C.} \quad (37)$$

The Eq. (36) represents the regime conditions of the AMRR, while the Eq. (37) represents the thermodynamic consistency. An iterative resolution of the Eqs. (2) and (19) provides the regime solution utilizing a tentative profile temperature of the magnetic bed

$$T_B(0,x) = T_{tr}(x) \quad (38)$$

The calculative cycle stops when the error δ reported below is smaller than 1×10^{-6} K:

$$\delta = Max\{|T_B(0,x) - T_B(t_D + t_{CF} + t_M + t_{HF},x)|\} \quad (39)$$

When the iterations stop the refrigeration energy and the energy supplied to the environment are calculated according to the following equations:

$$Q_{ref} = \int_{t_D}^{t_D + t_{CF}} \dot{m}(t)\bar{c}_f(T_c - T_f(t,0))dt \quad (40)$$

$$Q_{rej} = \int_{t_D + t_{CF} + t_M}^{t_D + t_{CF} + t_M + t_{HF}} \dot{m}(t)\bar{c}_f(T_f(t,L) - T_H)dt \quad (41)$$

To evaluate the mean powers it is necessary to consider the total cycle time:

$$\bar{\dot{Q}}_{ref} = Q_{ref}\frac{1}{t_{tot}} \quad (42)$$
$$\bar{\dot{Q}}_{rej} = Q_{rej}\frac{1}{t_{tot}} \quad (43)$$

Using these equations the coefficient of performance is evaluated:

$$COP_1 = \frac{Q_{ref}}{Q_{rej} - Q_{ref}} \quad (44)$$

The presented model do not take into account the work of the pump.

The Ergun equation [47] reported below allows the evaluation of the pressure drop in secondary fluid flow:

$$\frac{\partial p}{\partial x} = 180\left(\frac{1-\varepsilon}{\varepsilon}\right)^2 \frac{\mu_f}{d_p} w_{inf} + 1.8\left(\frac{1-\varepsilon}{\varepsilon^2}\right)\frac{\rho_f}{d_p} w_{inf}^2 \quad (45)$$

Integrating Eq. (45) along the magnetic bed with regard to the time, the pressure drop is evaluated. The work of the pump can be expressed as:

$$W_p = \frac{\dot{m}(t)(\Delta p_{CF} + \Delta p_{HF})}{\eta_p \rho_f}(t_{CF} + t_{HF}) \quad (46)$$

Using these equations the coefficient of performance is valuable:

$$COP_2 = \frac{Q_{ref}}{Q_{rej} - Q_{ref} + W_p} \quad (47)$$

5. Results and discussion

By means of the simulation with the previous equations, integrated with the boundary and the initial conditions, the refrigeration power, the coefficient of performance and the temperature profile of the magnetic bed have been obtained. In the simulation two temperature range have been explored: 260–280 K and 275–295 K. In the range 260–280 K the Gd–Dy alloys have been chosen as constituent materials for the regenerator. In the range 275–295 K the Gd–Tb alloys have been chosen as constituent materials for the regenerator.

In order to correctly design an AMRR cycle an optimization of the design parameters is mandatory. To this aim a sensitivity analysis has been carried out to evaluate the effect of layering bed on cycle performance.

The numerical program simulates layered regenerators made of $Gd_x\,Dy_{1-x}$ and $Gd_{-x}Tb_{1-x}$ alloys. The Curie temperature of the alloy varied with the change of the fraction of the two components. Therefore it is possible to make the bed of different numbers of layer each working at its optimal point selecting the composition of the alloy.

An iterative procedure has been adopted in order to determine the optimal composition of each layer of the bed. The procedure consists in the following steps:

(i) the bed consists in a predetermined number of layers of the same thickness of different alloy's composition (i.e. of different x);
(ii) a first tentative linear temperature profile has been assumed to hold in the bed ranging from T_c to T_h;
(iii) correspondingly a first trial bed composition has been assumed, in such a way that the Curie temperature of each layer equals the mean value of the two limit temperature of the layer;
(iv) a new temperature profile is evaluated by the simulation program based on the composition above;
(v) steps (iii) and (iv) are iterated until each layer contains its Curie temperature.

Table 3
Model parameters.

Characteristics	Values	Dimensions
d_p	600	μm
L	0.2	m
D	0.045	m
$\dot{Q}_{ref}$	105	W
B_{min}	0	T
B_{max}	1.5	T
$t_D = t_M$	0.2	s
$t_{CF} = t_{HF}$	2	s
T_h	280	K
T_C	260	K

The parameters reported in Table 3 are used to carry out the simulation to investigate the effect on cycle performance of layering bed with Gd–Dy alloys. In the simulation the cooling capacity was held constant selecting the appropriate regenerating fluid mass flow rate.

In Fig. 1 is reported as an example the Gd_xDy_{1-x} bed for a 6 layers bed varying the composition of the alloy.

Fig. 2 shows the COP_1 values varying the number of the bed's layer. In the graph the zero layer is referred to a bed make of pure Gd. The COP pertaining to a bed made of Gd is low because the Curie temperature is out of the temperature range. In the graph is reported the maximum COP referred to the Carnot cycle and the COP of a vapour compression plant working with the same operating conditions. In this Fig. 1 are reported COP values with three different secondary fluids: water–monoethylenglycol mixture (50% by weight), water–monoethylenglycol mixture (34% by weight) and water-1,2 propylenglycol mixture (38% by weight).

The COP_1 of the AMRR cycle is an increasing function of the layer's number. Indeed, increasing the layers of Gd–Dy alloys, placing each layer at the location where the average temperature is near its Curie temperature, a larger magnetocaloric effect can be obtained. Beyond 6 layers the COP_1 increases slightly. The non layered bed significantly out performs the layered bed and the COP is similar to that of a vapour compression plant.

The COP_1 values, for each number of layers, are similar between the three different secondary fluids used in the simulation. The water-1,2 propylenglycol mixture (38% by weight) shows COP_1 values slightly better than the water–monoethylenglycol mixture (34% by weight) (by a mean factor of +10%) and the water–monoethylenglycol mixture (50% by weight) (by a mean factor of +19%). Indeed, the greater values of the specific heat and of the thermal conductivity of this fluid allow a better heat exchange between the magnetic material and the regenerating fluid.

Comparing the value of the best COP_1 of an 8 layers AMRR cycle with that pertinent to a classical vapour compression plant, the AMRR shows an energetic performance greater than 63%.

In Fig. 3 is reported the adiabatic temperature variations of the 1 layer bed along the abscissa x during the magnetization and demagnetization. Along the magnetic bed in each phase a maximum variation of the adiabatic temperature is evidenced corresponding to the Curie temperature of the alloy.

In Fig. 4 is reported the adiabatic temperature variations of the 6 layer bed along the abscissa x during the magnetization and

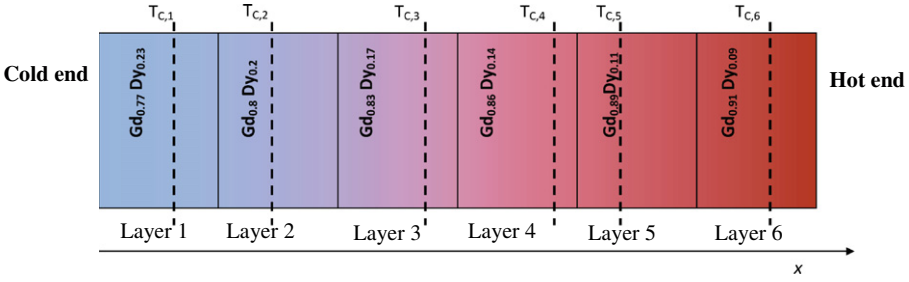

Fig. 1. Arrangement of the Gd_xDy_{1-x} alloys in a 6 layers AMRR bed.

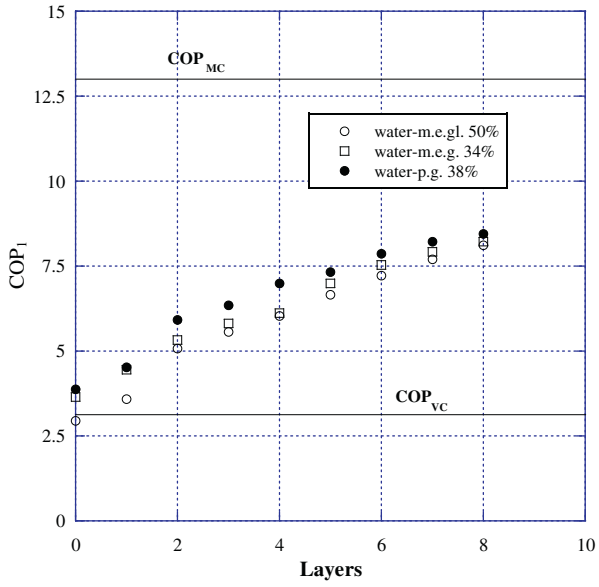

Fig. 2. COP_1 as a function of the layer's number with Gd_xDy_{1-x} alloys.

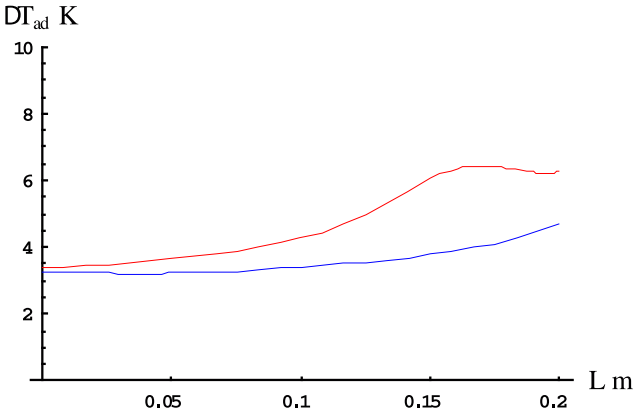

Fig. 3. Adiabatic temperature variation in a 1 layer Gd–Dy bed.

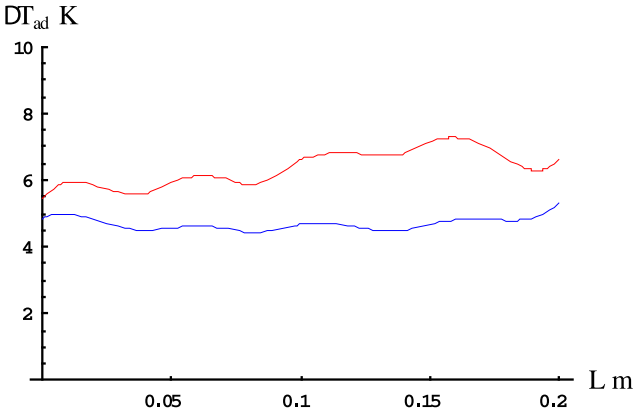

Fig. 4. Adiabatic temperature variation in a 6 layers Gd–Dy bed.

demagnetization. Along the magnetic bed a maximum variation of the adiabatic temperature is evidenced corresponding to Curie temperature of the alloy placed in each layer. In this case the bed works with greater adiabatic temperature variations and therefore with a greater magnetocaloric effect producing an increase of the energetic performance of the cycle.

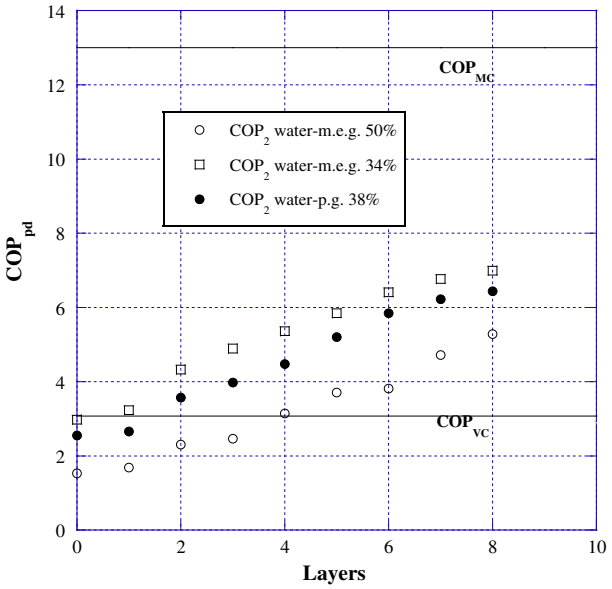

Fig. 5. COP_{pd} as a function of the layer's number with Gd_xDy_{1-x} alloys.

Table 4
Model parameters.

Characteristics	Values	Dimensions
d_p	600	μm
L	0.2	m
D	0.045	m
$\overline{Q}_{ref}$	105	W
B_{min}	0	T
B_{max}	1.5	T
$t_D = t_M$	0.2	s
$t_{CF} = t_{HF}$	2	s
T_h	295	K
T_C	275	K

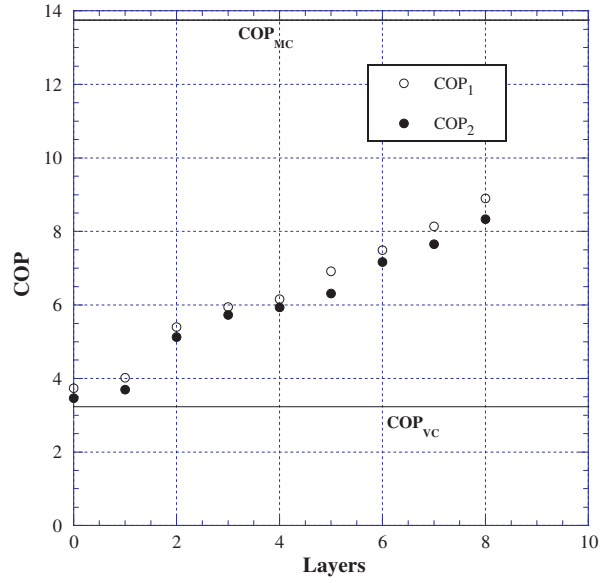

Fig. 6. COP_1 and COP_2 as a function of the layer's number with Gd_xTb_{1-x} alloys.

In Fig. 5 are reported the COP values taking into account the work of the pump. In the porous bed the pressure drops are very strong, therefore the work of the pump is significant and the COP

values decreases significantly taking into account the latter contribution. The viscosity of the water–monoethylenglycol mixture (50% by weight) is greater than that pertaining to the other secondary fluids tested in this analysis. Therefore with a greater work of the pump, the COP_2 values are much lower. Indeed, the COP of the AMRR cycle working with this mixture as secondary fluid is higher than that of a vapour compression plant only with a regenerator made of a number of layers >4. The best secondary fluid is water–monoethylenglycol mixture (34% by weight). With this fluid the AMRR cycle always over-performs a vapour compression cycle (from a minimum of +4 to a maximum of +59%).

The parameters reported in Table 4 are used to carry out the simulation to investigate the effect on cycle performance of layering bed with Gd–Tb alloys in the temperature range 275–295 K. In this temperature range the best secondary fluid is pure water. Indeed, this fluid is less viscous (with a lower work of the pump) and with higher values of specific heat and of thermal conductivity.

Fig. 6 shows the COP_1 and COP_2 values varying the number of the bed's layer. In the graph the zero layer is referred to a bed make of pure Gd. In the graph is reported the maximum COP referred to the Carnot cycle and the COP of a vapour compression plant working with the same operating conditions.

With water as a secondary fluid the work of the pump is negligible and COP_1 and COP_2 values are similar.

The non layered bed significantly out performs the layered bed but the COP is always better than that of a vapour compression plant. Comparing the value of the COP of an 8 layers AMRR cycle with that pertinent to a classical vapour compression plant, the AMRR shows an energetic performance >63%.

The parameters reported in Table 5 are used to carry out the simulation to investigate the effect on cycle performance of the regenerator volume with Gd–Dy alloys in the temperature range 260–280 K.

Fig. 7 illustrates the predicted COP_2 as a function of regenerator volume for a 6 layers bed and for a non layered bed; these curves were generated using a refrigeration capacity of 105 W and the optimal aspect ratio for each volume. In the figure is also reported the equivalent mass of the magnetic material. The secondary fluid used in this simulation is water–monoethylenglycol mixture (34% by weight). In figure is reported the coefficient of performance of a typical vapour compression plant in the same operating conditions. Fig. 7 indicates that an AMRR cycle with a 6 layer bed always is capable of achieving higher values of COP_2 than an equivalent vapour compression cycle (from a minimum of +11% to a maximum of +53%). A non layered bed has a better COP_2 only for a volume greater than 0.24 l (or a regenerator mass greater than 1.32 kg). As the AMRR regenerator increases, the operating efficiency increases. Indeed, increases the magnetocaloric effect of the magnetic material and decreases the secondary fluid mass to achieve the requested refrigeration capacity. Beyond a regenerator volume greater than about 0.35 l the COP_2 increases slightly and after begins to decrease. Indeed, the pressure drops increase with the length of the regenerator more than the decrease of the secondary fluid mass, increasing the work of the pump. The layered

Table 5
Model parameters.

Characteristics	Values	Dimensions
d_p	600	μm
$\overline{Q}_{ref}$	105	W
B_{min}	0	T
B_{max}	1.5	T
$t_D = t_M$	0.2	s
$t_{CF} = t_{HF}$	2	s
T_h	280	K
T_C	260	K

Table 6
Model parameters.

Characteristics	Values	Dimensions
d_p	600	μm
$\dot{Q}_{ref}$	105	W
B_{min}	0	T
B_{max}	1.5	T
$t_D = t_M$	0.2	s
$t_{CF} = t_{HF}$	2	s
T_h	295	K
T_C	275	K

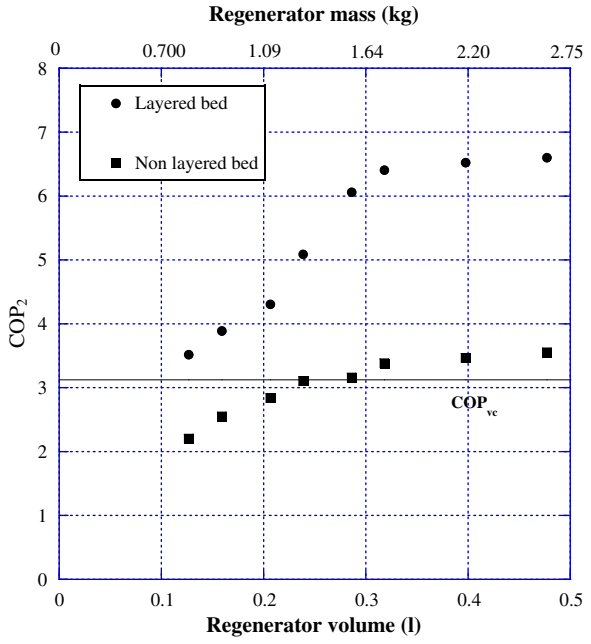

Fig. 7. COP_2 as a function of the regenerator's volume with Gd_xDy_{1-x} alloys.

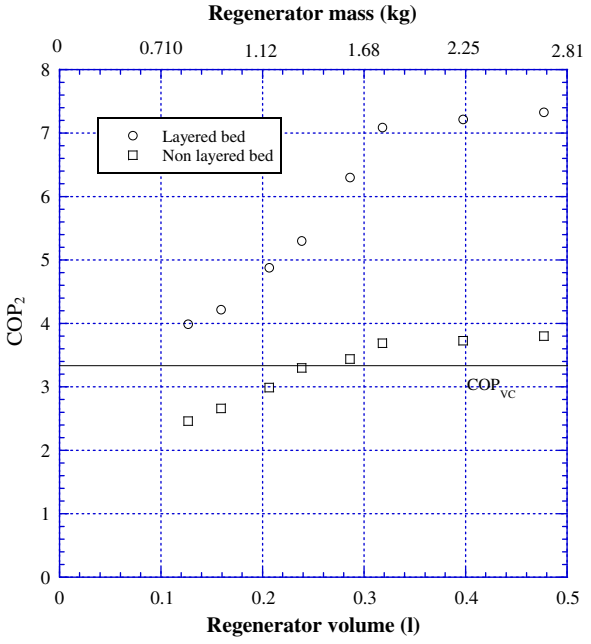

Fig. 8. COP_2 as a function of the regenerator's volume with Gd_xTb_{1-x} alloys.

bed significantly over-performs the non layered bed for any volume.

The parameters reported in Table 6 are used to carry out the simulation to investigate the effect on cycle performance of the regenerator volume with Gd–Tb alloys in the temperature range 275–295 K.

Fig. 8 illustrates the predicted COP_2 as a function of regenerator volume for a 6 layers bed and for a non layered bed; these curves were generated using a refrigeration capacity of 105 W and the optimal aspect ratio for each volume. In the figure is also reported the equivalent mass of the magnetic material. The secondary fluid used in this simulation is water. Fig. 8 indicates that an AMRR cycle with a 6 layer bed always is capable of achieving higher values of COP_2 than an equivalent vapour compression cycle (from a minimum of +17% to a maximum of +54%). A non layered bed has a better COP_2 only for a volume greater than 0.24 l. The layered bed significantly over-performs the non layered bed for any volume.

6. Conclusions

A numerical model of an AMRR has been developed. The model simulates both the ferromagnetic material and the entire cycle of an AMRR operating in conformity with a Brayton regenerative cycle.

The model predicts the refrigeration capacity and the efficiency of the cycle.

The Gd–Dy alloys have been chosen as constituent materials for the regenerators operating over the temperature range 260–280 K, whereas, the Gd–Tb alloys have been chosen as constituent materials for the regenerators operating over the temperature range 275–295 K. These materials have a very convenient property to produce layered beds, namely that the Curie temperature changes with the fraction of change of two components. The secondary fluids in the simulation are: water–monoethylenglycol mixture (50% by weight), water–monoethylenglycol mixture (34% by weight) and water-1,2 propylenglycol mixture (38% by weight) in the 260–280 K temperature range; pure water in the 275–295 K range.

In the present paper, a sensitivity analysis has been carried out to evaluate the effect of layering bed on cycle performance.

From the simulation the following conclusions can be drawn:

(1) The COP of the AMRR cycle is an increasing function of the layer's number. Indeed, increasing the layers of Gd–Dy and Gd–Tb alloys a larger magnetocaloric effect can be obtained and therefore a larger COP of the AMRR cycle. The non layered bed significantly out performs the layered bed with a COP that is similar or lower than that of a vapour compression plant. Comparing the value of the COP of an 8 layers AMR cycle with that pertinent to a classical vapour compression plant, the AMR shows an energetic performance >60–65%.

(2) Taking into account the work of the pump, the COP decreases strongly in the temperature range 260–280 K. Indeed, in the porous bed the pressure drops are very strong, therefore the work of the pump is significant. In the temperature range 275–295 K pure water can be used as secondary fluid and the work of the pump is less determinant.

(3) The best secondary fluid is water–monoethylenglycol mixture (34% by weight) in the temperature range 260–280 K. With this fluid the AMRR cycle always over-performs a vapour compression cycle (from a minimum of +4 to a maximum of +59%). Water is the best secondary fluid in the 275–295 K and the AMRR cycle always over-performs a vapour compression cycle (from a minimum of +2 to a maximum of +65%).

(4) The COP of an AMRR cycle depends strongly on the volume of the magnetic regenerator bed. As the volume increases, the operating efficiency increases. The layered bed always over-performs a non layered bed for each volume for Gd–Dy and Gd–Tb alloys.

These results indicate that this promising refrigeration technology will be used in chiller applications The model presented is a good instrument to design a prototype of a layered bed magnetic refrigerator working in conformity with a Brayton cycle.

References

[1] Zimm C, Jastrab A, Stenberg A, Pecharsky VK, Gschneidner Jr KA, Osborne M, et al. Handbook of heat transfer. New York, NY: McGraw-Hill; 1985. 6, pp. 10–1.
[2] Yu BF, Gao Q, Zhang B, Meng XZ, Chen Z. Review on research of room temperature magnetic refrigeration. Int J Refrig 2003;26:622–36.
[3] Pecharsky VK, Gschneiner KA. Magnetoaloric effect and magnetic refrigeration. J Magn Magn Mater 1999;200:44–56.
[4] Dan'kov SY, Tishin AM, Percharsky VK, Gschneidner KA. Magnetic phase transitions and the magnetothermal properties of gadolinum. Phys Rev B 1998;57(6):3478–90.
[5] Fujieda S, Hasegawa Y, Fujita A, Fukamichi K. Thermal Transport Magnetic Refrigerants $La(Fe_xSi_{1-x})_{13}$ and their hydbrides, and $Gd_5Si_2Ge_2$ and MnAs. J Appl Phys 2004;95(2):2429–31.
[6] Gschneidner Jr KA, Percharsky VK. The influence of magnetic field on thermal properties of solids. Mater Sci Eng 2000;287:301–10.
[7] Dai W, Shen BG, Li DX, Gao ZX. New magnetic refrigeration materials for temperature range from 165 K to 235 K. J Alloys Compd 2000;311:22–7.
[8] Nikitin SA, Andreyenko AA, Tishin AM, Arkharov AM, Zheredev AA. Magnetocaloric effect in Rare heart Alloys Gd–Ho, and Gd–Er. Phys Methals Metall 1985;59(2):104–8.
[9] Warburg E. Magnetische Untersuchungen. Über einige Wirkungen der Coërcitivkraft Magnetic investigations. A study of the effects of the coercive force. Ann Phys 1881;13:141–64.
[10] Brown GV. Magnetic heat pumping near room temperature. J Appl Phys 1976;47(8):3673–80.
[11] Green G, Patton G, Stevens J, Humphrey J. In: Reciprocating of the fourth international cryocoolers conference, Easton (MD); 1986.
[12] Rowe A, Tura A. Experimental Studies of Near Room temperature Magnetic Refrigeration. Int J Refrig 2006;29(8):1286–93.
[13] Rowe A, Tura A, Richard A, Chahine R, Barclay J. An overview of operating experience using the AMR test apparatus. Adv Cryogenic Eng 2004;49:1721–8.
[14] Rowe A, Tura A. Experimental investigation of a three-material layered active magnetic regenerator. Int J Refrig 2006;29(8):1286–93.
[15] Hirano N, Nagaya S, Takahashi M, Kuriyama T, Ito K, et al. Development of magnetic refrigerator for room temperature application. Adv Cryogenic Eng 2002;47:1027–34.
[16] Zimm C, Jastrab A, Sternberg A, Pecharsky V, Gschneidner K, Osborne M, et al. Description and performance of a near room temperature magnetic refrigerator. Adv Cryogenic Eng 1998;43:1759–66.
[17] Zimm C, Boeder A, Chell J, Sternberg A, Fujita S, Fujieda S, et al. Design and performanceof a permanent magnet rotary refrigerator. Int J Refrig 2006;29(8):1302–6.
[18] Zimm C, Boeder A, Chell J, Russek S, Sternberg A. Design and initial performance of magnetic refrigerator with a rotating permanent magnet. In: Second international conference on magnetic refrigeration at room temperature, Portoz, Slovenia; 2007.
[19] Clot P, Viallet D, Allab F, Kedous-Lebouc A, Fournier JM, Yonnet JP. A magnet based device for active magnetic regenerative refrigeration. IEEE Trans Magn 2003;39(5):3349–51.
[20] Lu DW, Xu XN, Wu HB, Jin X. A Permanent magnet magneto-refrigerator study on using Gd/Gd–Si–Ge/Gd–Si–Ge–Ga Alloys. In: First international conference on magnetic refrigeration at room temperature, Montreaux, Switzerland; 2005.
[21] Okamura T, Rachi R, Hirano N, Nagaya S. Improvements of 100 W class room temperature, Portoz, Slovenia; 2007.
[22] Yu BF, Gao Q, Zhang B, Meng XZ, Chen Z. Review on research of room temperature magnetic refrigerant. Int J Refrig 2003;26:622–36.
[23] Gao Q, Yu BF, Wang CF, Zhang B, Yang DX, Zhang Y. Experimental investigation on refrigeration performance of a reciprocating active regenerator of room temperature magnetic refrigeration. Int J Refrig 2006;29:622–36.
[24] Gschneidner Jr KA, Pecharsky VK. Thirty years of near room temperature magnetic cooling: where we are today and future prospects. Int J Refrig 2008;31(6):945–61.
[25] Engelbrecht KL, Nellis GF, Klein SA, Boeder AM. Modeling active magnetic regenerative refrigeration systems. In: First IIF–IIR international conference on magnetic refrigeration at room temperature, Montreaux, Switzerland; September 2005, p. 27–30.
[26] Engelbrecht KL, Nellis GF, Klein SA. Comparing modelling predictions to experimental data for active magnetic regenerative refrigeration systems. In:

Second IIF–IIR international conference on magnetic refrigeration at room temperature, Portoz, Slovenia; April 2007, p. 11–3.
[27] Dikeos J, Rowe A. Regenerator optimization through the numerical analysis of an active magnetic regenerator (AMR) refrigeration cycle. In: Weisend J et al., editors. Advances in Cryogenic Engineering, vol. 51. New York: AIP; 2006. p. 993–1000.
[28] Pekosoy O, Rowe A. Demagnetizing effect in active magnetic regenerators. J Magn Magn Mater 2005;288:424–32.
[29] Rowe A, Tura A. Active magnetic regenerator performance enhancement using passive magnetic materials. J Magn Magn Mater 2007;320:1357–63.
[30] Shir F, Mavriplis C, Bennett LH, Della Torre E. Analysis of room temperature magnetic regenerative refrigeration. Int J Refrig 2005;28:616–27.
[31] Allab F, Kedous-Lebouc A, Fournier JM, Yonnet JP. Numerical modelling for active magnetic regenerative refrigeration. IEEE Trans Magn 2005;41(10): 3757–9.
[32] Bouchekara H, Kedous-Lebouc A, Dupuis C, Allab F. Prediction et optimisation of geometrical properties of the refrigerant bed in an AMRR cycle. Int J Refrig 2008;31(7):1224–30.
[33] Petersen TF, Pryds N, Smith A, Hattel J, Schmidt H, Høgaard Knudsen H. Two-dimensional mathematical model of a reciprocating room-temperature active magnetic regenerator. Int J Refrig 2008;31:432–43.
[34] Nielsen KK, Bahl CRH, Smith A, Bjørk R, Pryds N, Hattel J. Detailed numerical modelling of a linear parallel-plate Active Magnetic Regenerator. Int J Refrig 2009;32:1478–86.
[35] Bouchard J, Nesreddine H, Galanis N. Model of a porous regenerator used for magnetic refrigeration at room temperature. Int J Heat Mass Transfer 2009;52:1223–9.
[36] Petersen TF, Engelbrecht K, Bahl C, Elmegaard B, Pryds N, Smith A. Comparison between a 1D and a 2D numerical model of an active magnetic regenerative refrigerator. J Phys D: Appl Phys 2008;41:105002–10.
[37] Bozoroth RM. Energy, specific heat, and magnetocaloric effect, ferromagnetism. New Jersey: D. Van Nostrand Company; 1956. p. 729–44.
[38] Shir F, Della Torre E, Bennett LH, Mavriplis C, Shull RH. Modelling of magnetization and demagnetization in magnetic regenerative refrigeration. IEEE Trans Magn 2004;40:2098–100.
[39] Tishin AM, Spichkin YI. The magnetocaloric effect and its applications. Inst Phys Publ Bristol Phila 2003:13–4.
[40] Aprea C, Maiorino A. A flexible numerical model to study an active magnetic refrigerator for near room temperature applications. Appl Energy 2010;87: 2690–8.
[41] Peksoy O, Rowe A. Demagnetization effects in active magnetic regenerators. J Magn Magn Mater 2005;288:424–32.
[42] Yu B, Gao Q, Yang D, Zhang Y. Research on performance of regenerative room temperature magnetic refrigeration cycle. In: Refrigeration science and technology proceedings of the international conference on magnetic refrigeration at room temperature, Montreaux; 2005, p. 9–68.
[43] Smaili A, Chahine R. Thermodynamic investigations on optimum active magnetic regenerators. Cryogenic 1998;38:247–52.
[44] Balli M, Allab F, Dupuis C, Fruchart D, Gignoux D, Kedous-Lebouc A, et al. Analysis and modelling of magnetocaloric effect near magnetic phase transition temperature. Second IIF–IIR international conference on magnetic refrigeration at room temperature, Portozm, Slovenia; 11–13 April 2007.
[45] Balli M, Fruchart D, Gignoux D, Miraglia S, Hlil EK, Wolfers P. Modelling of the magnetocaloric effect in $Gd_{1-x}Tb_x$ and MnAs compounds. J Magn Magn Mate 2007;316:558–61.
[46] Rohsenow WM, Hartnett JP, Ganic ENI. Handbook of heat transfer, vol. 6. New York: McGraw-Hill; 1985. p. 10–1.
[47] Kaviany M. Principles of heat transfer in porous media. New York: Springer; 1995 [p. 33, 46–7, 130, p. 28–9].